A&A 415, 549–558 (2004)
DOI: 10.1051/0004-6361:20034632
© ESO 2004

Astronomy & Astrophysics

High-frequency polarization properties of southern Kühr sources

R. Ricci[1,2], I. Prandoni[3], C. Gruppioni[4], R. J. Sault[2], and G. De Zotti[1,5]

[1] SISSA/ISAS, Via Beirut 2–4, 34014 Trieste, Italy
[2] Australia Telescope National Facility, CSIRO, PO Box 76, Epping, NSW 2121, Australia
[3] Istituto di Radioastronomia, CNR, Via Gobetti 101, 40129, Bologna, Italy
[4] INAF, Osservatorio Astronomico di Bologna, Via Ranzani 1, 40126 Bologna, Italy
[5] INAF, Osservatorio Astronomico di Padova, Vicolo dell'Osservatorio 5, 35122 Padova, Italy
e-mail: dezotti@pd.astro.it

Received 5 August 2003 / Accepted 21 November 2003

Abstract. We have observed 250 of the 258 southern sources in the complete 5 GHz 1 Jy sample by Kühr et al. (1981) using the Australia Telescope Compact Array (ATCA) at 18.5 GHz. This paper focuses on the polarization properties of this sample, while other properties will be addressed in a future paper. The analysis subdivides the sample into flat and steep spectrum sources using the classification of Stickel et al. (1994), where spectral indices were measured between 2.7 and 5 GHz. The polarized flux has been measured with a $S/N > 5$ for 170 sources (114 flat-spectrum and 56 steep-spectrum). Upper limits have been set for additional 27 sources (12 flat-spectrum and 15 steep-spectrum). The median fractional polarization at 18.5 GHz for the flat-spectrum sub-sample is $\Pi_{18.5} \simeq 2.7\%$, which is about a factor of 2 higher than at 1.4 GHz ($\Pi_{1.4} \simeq 1.4\%$, based on NVSS data). No evidence was found of significant correlations of the fractional polarization with other source properties. The median value of $\Pi_{18.5}$ for the steep spectrum sources is $\simeq$4.8%, but our sample might be biased against extended sources. We find some correlation between $\Pi_{18.5}$ and both the low-frequency (1.4–5 GHz) and the high-frequency (5–18.5 GHz) spectral indices. An important application of this work is in estimating the contamination of CMB polarization maps by extragalactic radio sources. Our results indicate that such contamination is within that estimated by Mesa et al. (2002).

Key words. radio continuum: galaxies – galaxies: nuclei – quasars: general – BL Lacertae objects: general – surveys

1. Introduction

Measurements of polarization properties of extragalactic radio sources provide unique information on magnetic field structure. The fractional polarization is a measure of the orderedness of the magnetic field in the emitting region. If synchrotron self-absorption and Faraday rotation can be neglected, the position angle will be orthogonal to the magnetic field orientation. Given this, it is surprising that high radio frequency polarimetric surveys of *complete* samples of extragalactic radio sources are so rare.

The general high-frequency polarization properties of radio sources are poorly known. Multifrequency observations by Jones et al. (1985) and Rudnick et al. (1985) of 20 flat-spectrum sources ($\alpha < 0.5$; $S \propto \nu^{-\alpha}$) showed that the median value of polarization is ~2.5% in the range 1.4–90 GHz, independent of frequency. This would suggest that the general polarization properties can be accounted for by largely random magnetic fields. Note, however, that Jones et al. and Rudnick et al. stressed that their sample is not complete and selection criteria may introduce unpredictable biases. On the other hand, the relatively constant polarization fraction suggests that differential Faraday rotation, or decreased contribution of relatively unpolarized opaque regions, or greater magnetic field ordering on the smaller scales dominating at millimeter wavelengths, may play minor roles (see also Saikia & Salter 1988). Okudaira et al. (1993) made linear polarization observations at 10 GHz for a complete sample of 93 flat-spectrum sources selected at 5 GHz ($S_{5\ \mathrm{GHz}} > 0.8$ Jy). Okudaira et al. do not provide an average value for the fractional polarization at 10 GHz. From their tabulated source values one could infer a median fractional polarization of 2.3%. On the other hand, Aller et al. (1999) find that the fractional linear polarization of a incomplete sample of 41 BL Lac objects is generally higher at 14.5 GHz (median value 5%) than at 4.8 GHz (median value 3.6%). Also, the millimeter/sub-millimeter polarization survey of 26 blazars by Nartallo et al. (1998) yielded a median fractional polarization at 0.8–1.1 mm of 7.1%, while the NVSS data indicate, for the same objects, a median fractional polarization of $\simeq$2% at 1.4 GHz (Mesa et al. 2002). For a sample of steep-spectrum sources with multifrequency polarimetric observations by Klein et al. (2003), Mesa et al. (2002) find a steady increase with frequency of the mean fractional polarization from $\simeq$3% at 1.4 GHz to 8.65% at 10.6 GHz. It should be noted, however, that the sample is biased towards high polarizations as it

Send offprint requests to: R. Ricci, e-mail: ricci@sissa.it

Article published by EDP Sciences and available at http://www.aanda.org or http://dx.doi.org/10.1051/0004-6361:20034632

includes only sources which have been detected in polarization at 10.6 GHz. The same effect may occur in the high redshift radio galaxy sample observed by Pentericci et al. (2000) at high resolution (0.″2), where typical fractional polarizations of 10–20% at 8.4 GHz were found.

A good understanding of the high-frequency polarization properties of extragalactic sources is crucial in analysing the polarization of the cosmic microwave background (CMB). This has been detected recently by the DASI experiment at 30 GHz (Kovac et al. 2002) and by the WMAP satellite (Kogut et al. 2003) in several bands in the range 23–94 GHz. The extraction of the very weak CMB polarization signal requires both high sensitivity and careful control of foregrounds. In the frequency range relevant to these experiments, the polarized emission of extragalactic radio sources is expected to be the main contaminant on small angular scales (Sazhin & Korolëv 1985; De Zotti et al. 1999).

In this paper we describe the results of linear polarization measurements at 18.5 GHz of 250 of the 258 southern ($\delta < 0°$) extragalactic sources in the 5 GHz Kühr et al. (1981) all-sky sample. This sample is complete to $S_{5\ \mathrm{GHz}} \geq 1$ Jy, and contains 527 objects. This is, by far, the largest *complete* sample of radio sources for which high-frequency polarization measurements have been carried out. Observations and data reduction are described in Sects. 2 and 3, respectively. The results are analyzed and discussed in Sect. 4. In Sect. 5 we summarize our main conclusions.

2. Observations

Measurements were carried out with the Australia Telescope Compact Array (ATCA). Since 2001 this facility has been undergoing a major millimeter upgrade that will provide 12 mm and 3 mm receivers on all the ATCA antennas. In the commissioning phase, prototype 12 mm receivers were mounted on antennas CA02, CA03 and CA04. We took snapshot observations of the southern sources in the so-called EW367 array configuration. The two frequency bands were centered at 18.5 and 18.65 GHz with each band having a bandwidth of 128 MHz. The array configuration that we used is quite compact: the longest baseline was 214.3 meters, giving a beamwidth of 15.6 arcsec.

The observations were performed in three runs during March 2002. The total observing time was 48 hours: 24 hours on March 20-21, 10 hours on March 21-22 and 14 hours on March 27-28. We used the "mosaic observing mode" because this allowed us to organize the observing sequence to minimize the slew time between the sources. The 258 sources were split in 36 clusters of sources. Clusters were observed four times each to produce a good spread in hour angles.

Many of these sources had already been targeted with the ATCA as part of a search for potential 22 GHz calibrators. The 22 GHz total intensity measurements with ATCA of the full sample were completed in January 2001; the results will be reported in a subsequent paper. These measurements were used to determine the integration time for each target source to ensure a detection at $\geq 5\sigma$ for source polarizations $\geq 1\%$. Nevertheless, because of limited observing time, we set an upper limit of 30 min per source. This means that for 43 sources with 22 GHz flux density ≤ 0.192 Jy, the detection threshold is $\geq 1\%$. Because of technical problems during the runs, 8 sources were not successfully observed.

3. Data reduction

The radio source 1934-638 was used as the primary flux density calibrator, while phase and gain calibrators were chosen from the ATCA calibrator list. The instrumental polarization was calibrated using measurements of Jupiter, which we assumed to be unpolarized.

Unfortunately the atmospheric phase stability during the observations was poor, so it was not possible to image the sources. Instead we decided to use non-imaging model-fitting techniques. To measure calibrators sufficiently frequently to correct for phase instability would have been quite expensive in time: this would have reduced significantly the number of sources that we could observe in the scheduled time.

The data were reduced in the MIRIAD software package (Sault et al. 1995) to derive source flux densities in all the Stokes parameters (I, Q, U, V). In particular we used the MIRIAD task CALRED to determine the flux densities. In processing the visibilities, CALRED assumes a point source model, and produces a flux density estimate for each Stokes parameter for *each scan*. Along with the flux density and its error, the task computes out the theoretical rms noise, and a confusion parameter, C. The confusion parameter is an estimate of the fraction of the flux density that fails to conform to a point-source model.

A high value of C means that the source is poorly modelled as a point and that the determination of its flux density is poor. On the other hand, even in the case of truly point sources (where the value of C should be 0), noise results in a spread of the estimated value of C. For normal error distribution, C is approximately described by a semi-Gaussian distribution (negative values of C are not allowed). The observed distribution of C (Fig. 1) shows a strong excess over the best-fit Gaussian curve where $C \geq 5\%$: we believe this is a result of source extension. Consequently we have chosen to exclude all the scans with $C \geq 5\%$. This resulted in the rejection of 53 sources.

For the remaining 197 sources we computed the linearly polarized flux for each scan i, $F_{\mathrm{p},i} = \sqrt{Q_i^2 + U_i^2}$ and the associated error $\sigma_{\mathrm{F},i} = \sigma_{Q,i} = \sigma_{U,i}$ ($\sigma_{Q,U}$ being the rms noise on the Stokes parameter Q or U). For all the sources the polarized flux, F_{p}, and its error, σ_{F}, were obtained by using a weighted mean over all the scans:

$$F_{\mathrm{p}} = \sigma_{\mathrm{F}}^2 \sum_i \frac{F_{\mathrm{p},i}}{\sigma_{\mathrm{F},i}^2} \tag{1}$$

$$\frac{1}{\sigma_{\mathrm{F}}^2} = \sum_i \frac{1}{\sigma_{\mathrm{F},i}^2}. \tag{2}$$

For 170 sources the polarized flux was detected with a signal-to-(theoretical)noise ratio ≥ 5. We considered such values as reliable. An upper limit of 5 $\times$ the theoretical noise was assigned to the other 27 sources. In all cases, the total intensity,

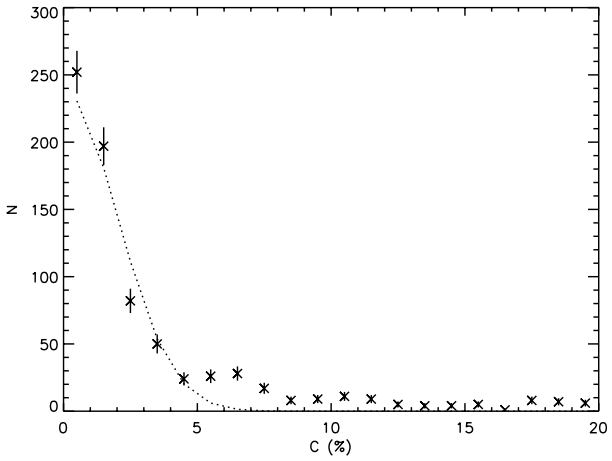

Fig. 1. Distribution of the confusion parameter C. A semi–Gaussian fit is also shown (dotted line). The fitted standard deviation is $\sigma = 2.03$.

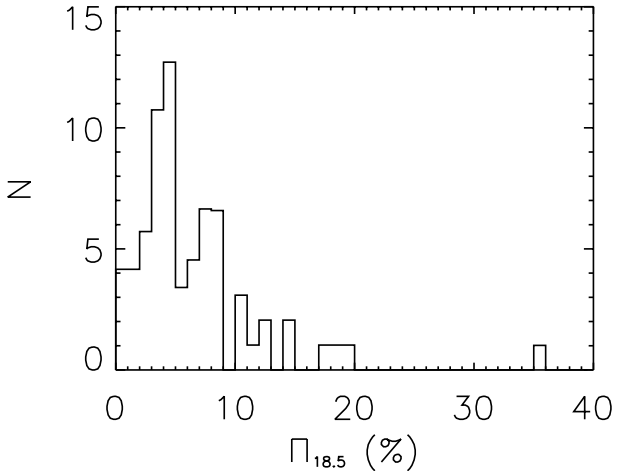

Fig. 2. Distribution of the fractional polarization at 18.5 GHz for the steep-spectrum sources.

Table 1. Source number statistics for the polarization observations. The fractions in brackets are the percentages of flat and steep spectrum sources.

	All	Flat		Steep	
detections	170	114	(80%)	56	(49%)
upper limits	27	12	(8%)	15	(13%)
rejected	53	13	(9%)	40	(35%)
not observed	8	4	(3%)	4	(3%)
total	258	143		115	

I (again derived as the weighted mean of the scan total intensities), was measured with very high S/N ratio. The observations did not determine the polarization position angle: the geometry on the ATCA 12 mm receivers was not calibrated sufficiently well to give reliable position angle information.

In the following analysis we subdivide the sample into flat and steep-spectrum sources. Following the classification of Stickel et al. (1994), we define as flat the sources with spectral index between 2.7 and 5 GHz $\alpha^5_{2.7} < 0.5$ ($S_\nu \propto \nu^{-\alpha}$). Sources with $\alpha^5_{2.7} > 0.5$ are considered steep. In Table 1 we list the number (and the corresponding fraction of the total) of detected sources for the flat and steep-spectrum sub-samples. For both classes we also list the upper limits and the rejected sources ($C > 5\%$). While the final flat-spectrum source sample is almost complete (88%), only 49% of the steep-spectrum sources have reliable detections.

The total intensities and polarized fluxes for steep and flat-spectrum sources are listed in Tables 5 and 6, respectively. Also listed are the linear fractional polarization $\Pi_{18.5} = F_\mathrm{p}/I$, the spectral indices between 1.4 and 5 GHz ($\alpha^5_{1.4}$) and 5 and 18.5 GHz ($\alpha^{18.5}_5$) and the 5 GHz luminosity. Source types and redshifts are from Stickel et al. (1994).

4. Polarization properties of sources

4.1. Steep-spectrum sources

As expected, most of the rejected sources (40 out of 53 with $C > 5\%$) are steep-spectrum. This is because steep-spectrum sources are more likely extended than flat-spectrum sources. This means that the following analysis is based on an incomplete sample, which can be strongly biased against extended sources (see Table 1). Additionally, only upper limits can be given for 15 out of 71 (∼21%) of the steep-spectrum sources. Nevertheless some points are worth noticing. In Fig. 2 we show the parent distribution of $\Pi_{18.5}$ for the steep-spectrum sample. This was obtained by using the Kaplan–Meier estimator (routine KMESTM in the software package ASURV Rev 1.2, (Isobe & Feigelson 1990). This includes upper limits by using the survival analysis methods presented in Feigelson & Nelson (1985) and Isobe et al. (1986)). The median of the distribution is ≃4.8% and the mean is ≃6.5 ± 0.7%. If we divide the sample into quasars (21 sources) and radio galaxies (50 sources) we find median values of 4.4% and 6.1%, and mean values of 5.1 ± 0.6% and 7.0 ± 0.9% respectively. The Peto & Prentice generalized Wilcoxon two sample test yields a probability of 21.7% that the distributions of QSOs and radio galaxies are drawn from the same parent population.

These values are somewhat lower than those found by Klein et al. (2003) at 10.6 GHz and by Pentericci et al. (2000) at 8.4 GHz by for their sample of high-redshift radio galaxies observed at high angular resolution (typical polarizations of 10–20%). Nevertheless we point out that both the high spatial resolution of the Pentericci et al. sample and the selection criterion used by Klein et al. may introduce a bias toward high fractional polarization values, as stressed in the introduction.

We have used the NVSS public data (Condon et al. 1998) to investigate the polarization properties of our sources at 1.4 GHz. The 37 steep-spectrum sources detected by the NVSS in the overlapping region, have a median 1.4 GHz fractional polarization of ≃0.4%, comparable to the residual instrumental polarization (0.3%). To obtain a more reliable estimate of the 1.4 GHz polarization, we included the steep-spectrum Kühr sources in the Northern sky. This selected 184 objects in total. We find $\Pi_{1.4,\mathrm{median}} \simeq 1.1\%$. The Peto & Prentice two-sample test rules out at a very high confidence level ($P < 10^{-5}$) the hypothesis that the distributions at 1.4 and 18.5 GHz are drawn from the same parent population.

Table 2. Test for correlations between $\Pi_{18.5}$ and other properties of the steep-spectrum sources. N is the number of sources, Z is the generalized Kendall's correlation coefficient and P is the probability that a correlation is not present.

Correlation	N	Z	P
$\Pi_{18.5} - \alpha_5^{18.5}$	71	3.526	0.0004
$\Pi_{18.5} - \alpha_{1.4}^{5}$	37	2.747	0.006
$\Pi_{18.5} - z$	49	1.283	0.1996
$\Pi_{18.5} - \log L_{5\ \mathrm{GHz}}$	27	0.764	0.445
$\Pi_{18.5} - \Pi_{1.4}$	37	0.526	0.5992

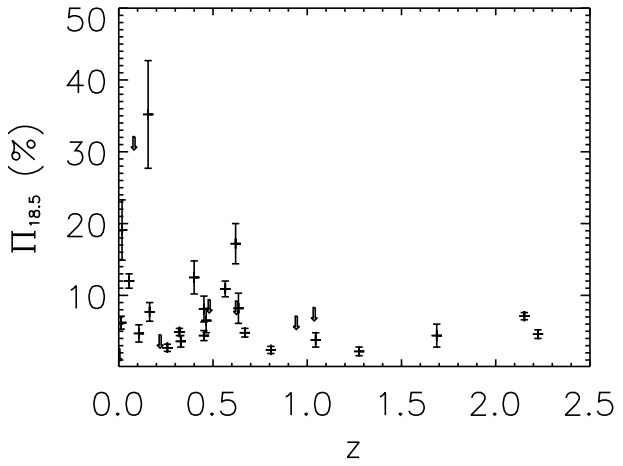

Fig. 3. $\Pi_{18.5}$ vs. redshift for the steep-spectrum sample. $\Pi_{18.5}$ upper limits are represented by downward arrows.

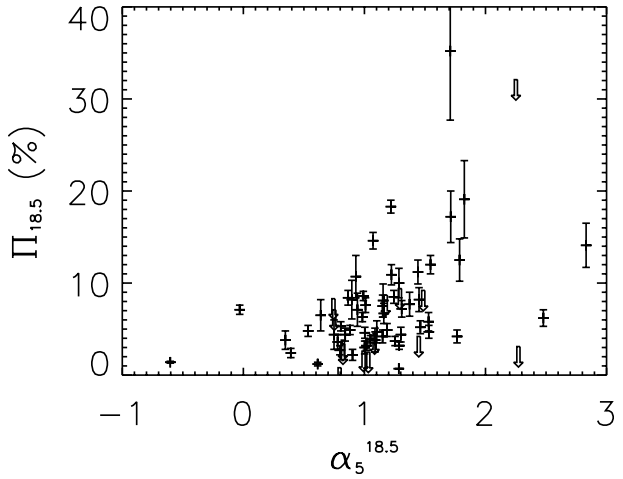

Fig. 4. $\Pi_{18.5}$ vs. $\alpha_5^{18.5}$ for the steep-spectrum sample. $\Pi_{18.5}$ upper limits are represented by downward arrows.

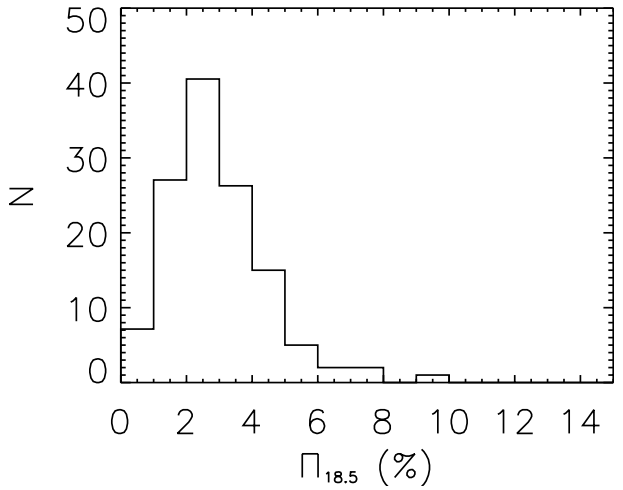

Fig. 5. Distribution of the fractional polarization at 18.5 GHz for the flat-spectrum sample.

The origin of this frequency dependence is not well understood. The multifrequency polarization measurements by Klein et al. (2003), quoted by Mesa et al. (2002), indicated an increase by a factor of $\simeq$3 of the fractional polarization of steep-spectrum sources between 1.4 and 10.4 GHz. This is attributed to Faraday depolarization in uniform slabs with effective rotation measure $RM \simeq 260\,\mathrm{rad\,m^{-2}}$. However, an increase of the fractional polarization with frequency, as expected in the case of a Faraday screen at the source, translates in a positive correlation with redshift. For example, in the presence of a Faraday screen located at redshift z, the observed rotation measure is related to the intrinsic value by $RM_{\mathrm{obs}} = RM_{\mathrm{intr}}(1+z)^{-2}$. However no significant correlation is found in our data between $\Pi_{18.5}$ and z (see Fig. 3 and Table 2). This may be consistent with the findings by Pentericci et al. (2000) that the fraction of powerful radio galaxies with extreme Faraday rotation measures ($RM > 1000\,\mathrm{rad\,m^{-2}}$) increases steeply with redshift. This suggests that their average environment becomes increasingly dense with increasing z. The larger mean fractional polarization measured at 18.5 GHz may imply that Faraday depolarization is negligible at high frequencies. Polarization measurements at intermediate frequencies are necessary to assess this.

Table 2 also shows the results of our investigation of possible correlations of $\Pi_{18.5}$ with other source properties. There are indications of a correlation with the spectral indices $\alpha_{1.4}^{5}$ and (more significantly) $\alpha_5^{18.5}$: steeper sources seem to have stronger $\Pi_{18.5}$ (Fig. 4). The fact that sources with the highest $\Pi_{18.5}$ and the steepest $\alpha_5^{18.5}$ are generally at low redshift may suggest that they are resolved and we are actually seeing highly polarized portions of them, such as radio lobes. We note, however, that any correlation should be taken with caution due to the incompleteness of the steep-spectrum source sample. The fractional polarizations at 18.5 and 1.4 GHz are uncorrelated. We do not see any correlation between fractional polarization and other source properties.

4.2. Flat-spectrum sources

We used the Kaplan-Meyer estimator to derive the fractional polarization distribution of the 126 flat-spectrum sources in our final sample (114 detections and 12 upper limits). The result is shown in Fig. 5: the median value is 2.7% and the mean value is $2.9 \pm 0.1\%$. This is about a factor of 2 lower than that found for the steep-spectrum sources.

We used the NVSS catalog (Condon et al. 1998) to determine the fractional polarization at 1.4 GHz, $\Pi_{1.4}$: 86 flat-spectrum sources overlap with the NVSS survey. The distribution of $\Pi_{1.4}$ is shown in Fig. 6: it has a median value of 1.4%,

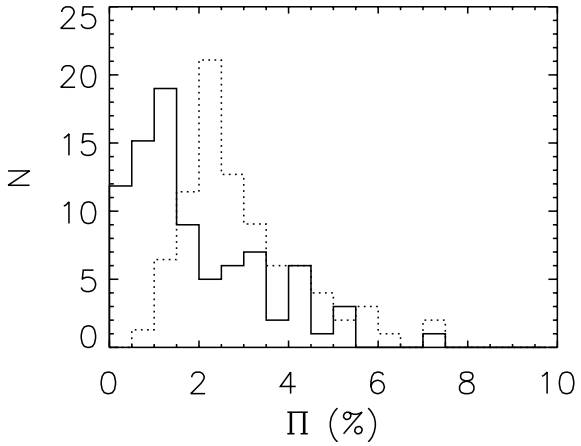

Fig. 6. Linear fractional polarization distribution at 1.4 GHz (solid line) and 18.5 GHz (dotted line) for the 86 flat-spectrum southern Kühr sources in the NVSS survey.

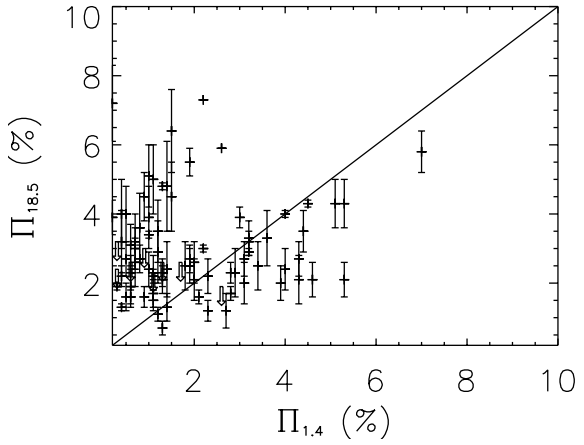

Fig. 7. $\Pi_{18.5}$ vs. $\Pi_{1.4}$ for the flat-spectrum sample. $\Pi_{18.5}$ upper limits are represented by downward arrows.

Table 3. Median fractional polarization of flat-spectrum sources. Columns 2 and 5 give the number and the median fractional polarization at 18.5 GHz of the different classes of sources in our sample. In parentheses are the number of such sources in the NVSS area (Col. 3), and their median fractional polarization at 18.5 GHz (Col. 6) and at 1.4 GHz (Col. 7). Columns 4 and 8 give the total number of Kühr flat-spectrum sources of the different classes in the NVSS catalog, and their median fractional polarization at 1.4 GHz.

Type		*N*		$\Pi_{18.5}$ (%)		$\Pi_{1.4}$ (%)	
QSO	108	(74)	175	2.7	(2.6)	(1.4)	1.4
BL Lac	8	(5)	34	3.0	(2.9)	(1.2)	2.2
GAL	8	(5)	25	2.4	(2.5)	(1.8)	0.3

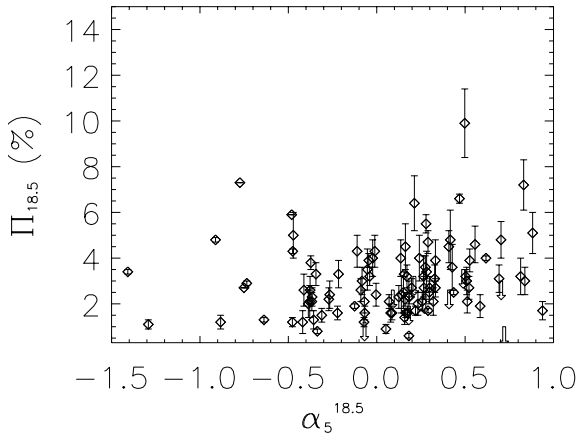

Fig. 8. $\Pi_{18.5}$ vs. $\alpha_5^{18.5}$ for the 108 flat-spectrum QSOs. $\Pi_{18.5}$ upper limits are indicated by downward arrows.

comparable to the value found for steep-spectrum sources, and a factor of 2 lower than that at 18.5 GHz. This seems to be in disagreement with the results of Jones et al. (1985) and Rudnick et al. (1985), who found a constant polarization value of 2.5% in the frequency range 1.4–90 GHz.

In Table 3 we give the median fractional polarization for different classes of objects in the flat-spectrum sample (QSOs, BL Lacs and radio galaxies). In the last column of the table, we give the median fractional polarization at 1.4 GHz that was computed by including the northern ($\delta > 0$) Kühr sources with NVSS detection. Adding the latter sources increases the total number of flat-spectrum sources with 1.4 GHz polarization data from 86 to 238: the number of QSOs increases from 74 to 175, that of BL Lacs from 5 to 34, and that of galaxies from 5 to 25. We do not find any significant indication of differences in the 18.5 GHz polarization properties of the various sub-populations. However the very small number of BL Lacs and radio galaxies means that this comparison is not very meaningful. The comparison at 1.4 GHz is more significant: the Peto & Prentice generalized Wilcoxon two sample test yields probabilities of $\simeq$1% and of 0.001% that the fractional polarization distributions of QSOs are drawn from the same parent population as BL Lacs and radio galaxies, respectively.

As illustrated in Fig. 7, sources that are weakly polarized at 1.4 GHz show a stronger fractional polarization at 18.5 GHz. This could be suggestive of differential Faraday depolarization effects. Nevertheless, we do not see an increase of the fractional polarization with redshift, as might be expected in the case of Faraday depolarization inside the source. It should be remembered that the emission at different frequencies comes from different regions in the source, and that these regions may have intrinsically different polarization properties. On the other end, sources with $\Pi_{1.4} \gtrsim 2\%$ tend to have $\Pi_{1.4} \gtrsim \Pi_{18.5}$, which may be the result of the decreased contribution, at high-frequency, of the more polarized, steep-spectrum, diffuse component.

To get further hints on mechanisms that determine the polarization properties of sources, we used the generalized Kendall's rank correlation coefficient Z to look for possible correlations between $\Pi_{18.5}$, $\Pi_{1.4}$ and other properties of our flat-spectrum radio sources, such as: the low-frequency spectral index (between 1.4 GHz and 5 GHz), the high-frequency spectral index (between 5 and 18.5 GHz), the monochromatic luminosity at 5 GHz. The values of the probability P that *no* correlation is present are given for both the whole flat-spectrum sample and the flat-spectrum QSOs only in Table 4. At variance with what found for the steep-spectrum sample, there is no significant evidence of a correlation between $\Pi_{18.5}$ and $\alpha_5^{18.5}$ (see Fig. 8).

Table 4. Test for correlations between the fractional polarization at 18.5 and 1.4 GHz and other properties of the flat-spectrum sources (whole sample and QSO sub-sample only). Z is the generalized Kendall's correlation coefficient and P is the probability that a correlation is not present.

Correlation	Z		P	
	All	QSO	All	QSO
$\Pi_{18.5} - \alpha_{1.4}^{5}$	0.47	0.23	0.48	0.63
$\Pi_{18.5} - \alpha_{5}^{18.5}$	1.83	2.29	0.07	0.02
$\Pi_{18.5} - z$	0.23	0.09	0.82	0.93
$\Pi_{18.5} - L_{5\ \mathrm{GHz}}$	0.91	0.56	0.36	0.58
$\Pi_{18.5} - \Pi_{1.4}$	0.95	0.24	0.34	0.81
$\Pi_{1.4} - \alpha_{1.4}^{5}$	0.89	0.89	0.38	0.37
$\Pi_{1.4} - \alpha_{5}^{18.5}$	1.90	1.47	0.05	0.14
$\Pi_{1.4} - z$	1.85	1.53	0.06	0.13
$\Pi_{1.4} - L_{5\ \mathrm{GHz}}$	1.75	1.58	0.08	0.11

5. Discussion and conclusions

We have performed high-frequency observations of a large, complete sample of bright extragalactic radio sources: 250 of the 258 sources in the southern sky ($\delta < 0°$) of the 5 GHz Kühr et al. (1981) sample were observed with the ATCA at 18.5 GHz. This sample is complete to $S_{5\ \mathrm{GHz}} \geq 1$ Jy. The polarized flux has been measured to better than 5σ for 170 sources (114 flat-spectrum and 56 steep-spectrum) and upper limits have been set for additional 27 sources (12 flat-spectrum and 15 steep-spectrum). This represents to 88% of the flat-spectrum sources and 62% of the steep-spectrum sources in the southern Kühr sample. 53 sources were not considered in our analysis, as they appear to be extended (i.e. our point-source model fitting technique showed a significant fraction of non-pointlike emission). Most of the extended sources are steep-spectrum. Consequently our conclusions about this class of objects may be biased against extended sources.

The median fractional polarization at 18.5 GHz for steep and flat-spectrum sources was found to be $\simeq$4.8% and $\simeq$2.7%, respectively. The distributions are both skewed, with tails towards high values, up to a maximum of $\simeq$20% and $\simeq$10%, respectively. That steep-spectrum sources generally display higher fractional polarization than flat-spectrum sources could be explained either in terms of different intrinsic polarization properties of the two classes of objects, or in terms of different internal depolarization effects (flat sources, usually dominated by their core emission, could be more heavily depolarized). An alternative to depolarization by internal Faraday rotation is also offered by gradients in an external Faraday screen that are not resolved by our observations. However, these two depolarizing mechanisms cannot be distinguished given polarization measurements at only two frequencies. Moreover, spectral indices and polarization levels of low redshift steep-spectrum radio sources with high polarization degrees ($\Pi_{18.5} > 10\%$) could be overestimated due to resolution effects. Magnetic fields are more ordered on small angular scales, thus increasing polarization degrees on those scales.

We used the NVSS survey data to derive the fractional polarization at 1.4 GHz for the Kühr all-sky sample. We find very similar median values for both the steep and the flat sources (1.1% and 1.4%, respectively). This means a factor of ~4 (~2) increase from 1.4 to 18.5 GHz for the steep (flat) spectrum sources. It is unclear whether such an increase can be attributed to a decreased internal Faraday depolarization. In this case we would expect the fractional polarization to be correlated with redshift. However such a correlation is not found either for the steep or for the flat spectrum sources. For steep-spectrum sources, any redshift dependence could be counteracted by a steep increase of the intrinsic Faraday rotation measures with redshift, reflecting an increase of the environmental density (Pentericci et al. 2000). For the flat-spectrum sample, on the other hand, it is more likely that the increase in polarization is because the radio emission at different frequencies comes from different core components, that may have intrinsically different polarization properties.

We do not see any significant correlation between $\Pi_{18.5}$ and other source properties, such as the low-frequency spectral index and the luminosity at 5 GHz. A possible weak (3σ) correlation between $\Pi_{18.5}$ and the high-frequency spectral index, $\alpha_5^{18.5}$, is apparent in the steep-spectrum sample only.

An important application of these results is in the estimate of the contamination of CMB polarization maps by extragalactic radio sources (Mesa et al. 2002). Based on the multifrequency radio polarimetry by Klein et al. (2003), Mesa et al. (2002) estimated an average increase by a factor of 3 of the fractional polarization of steep-spectrum sources from 1.4 GHz to higher frequencies. Our data suggest an increase by a larger factor (~4), although caution is needed because of the strong incompleteness of the steep-spectrum sample. On the other hand, it is worth noticing that steep-spectrum sources provide a minor contribution to polarization fluctuations at frequencies ($\gtrsim$ 30 GHz) where CMB measurements are carried out. For flat-spectrum sources, Mesa et al. (2002) considered two possibilities: that the fractional polarization remains, on average, constant from 1.4 GHz to high frequencies (as found by Rudnick et al. 1985), or increases by a factor of 3 (as found by Nartallo et al. 1998). Our results are intermediate (an increase of a factor of ~2). This suggests a contamination of CMB polarization maps which is likely to be within the ranges considered by Mesa et al. (2002).

Acknowledgements. This research was supported in part by the Italian Space Agency (ASI) and by the Italian MIUR through a COFIN grant. RR gratefully acknowledges a financial contribution from the Italian National Research Council (CNR) as part of an exchange program with CSIRO; he also warmly thanks the Paul Wild Observatory staff for their kind hospitality at Narrabri (NSW, Australia) where some of this work was completed. We are grateful to the referee for useful comments that helped improving the paper.

Table 5. Summary of observed and derived quantities for the steep spectrum sample: (1) source name (B1950); (2) observation dates (1 = March 20–21, 2 = March 22, 3 = March 27–28); (3) redshift; (4) source type; (5)–(6) 18.5 GHz total intensity and its error in mJy; (7)–(8) 18.5 GHz polarized flux and its error in mJy; (9)–(10) 18.5 GHz fractional polarization (%) and its error (%); (11) spectral index between 1.4 and 5 GHz; (12) spectral index between 5 and 18.5 GHz; (13) logarithm of the 5 GHz luminosity in W Hz^{-1}; (14) 1.4 GHz NVSS fractional polarization (%).

(1)	(2)	(3)	(4)	(5)	(6)	(7)	(8)	(9)	(10)	(11)	(12)	(13)	(14)
name	dates	z	type	I	σ_I	$F_{\rm p}$	$\sigma_{\rm F}$	$\Pi_{18.5}$	σ_Π	$\alpha_{1.4}^{5}$	$\alpha_{5}^{18.5}$	$\log L_5$	$\Pi_{1.4}$
0003−003	2, 3	1.03700	QSO	525.0	14.0	<43.5	8.7	<8.3	1.7	0.81	0.74	27.86	0.66
0008−421	1	...	EF	181.6	0.6	9.4	1.2	5.2	0.7	...	1.46	...	...
0022−423	1	...	QSO	339.9	0.6	10.9	1.4	3.2	0.4	...	1.28	...	...
0023−263	3	0.32200	GAL	1143.7	5.5	55.8	6.2	4.9	0.5	0.69	0.88	27.20	0.11
0035−024	2, 3	0.21970	GAL	651.0	14.0	<29.0	5.8	<4.5	0.9	0.65	1.08	26.73	0.20
0039−445	1	...	GAL	218.6	0.7	15.7	2.0	7.2	0.9	...	1.30	...	...
0042−357	1	...	NO ID	269.9	0.7	20.6	2.1	7.6	0.8	0.73	1.00	...	1.31
0045−255	2	0.00086	GAL	638.4	2.9	<16.6	3.3	<2.6	0.5	0.19	0.99	21.84	<0.10
0105−163	2, 3	0.40000	GAL	114.0	2.0	14.2	2.6	12.5	2.3	0.99	1.78	26.95	0.45
0114−211	2, 3	...	EF	280.5	1.7	18.9	3.1	6.7	1.1	0.91	1.16	...	0.10
0117−155	2, 3	0.56500	GAL	325.0	2.0	35.5	3.7	10.9	1.1	0.90	1.22	27.39	0.68
0123−016	2, 3	0.01770	GAL	170.0	6.0	32.4	7.1	19.1	4.2	...	1.82	...	...
0131−367	1	...	GAL	54.9	0.6	7.8	1.3	14.1	2.4	...	2.83	...	...
0159−117	2, 3	0.66900	QSO	690.0	5.0	33.1	4.4	4.8	0.6	0.53	0.53	27.40	3.52
0201−440	1	...	QSO?	256.0	1.4	37.3	2.4	14.6	0.9	...	1.07	...	...
0235−197	2	0.62000	GAL	154.1	1.0	26.5	4.3	17.2	2.8	0.91	1.71	27.43	2.93
0237−233	2	2.22400	QSO	915.8	3.5	42.0	5.9	4.6	0.6	0.47	1.00	28.78	0.83
0252−712	1	...	GAL	316.6	0.9	11.7	1.7	3.7	0.5	...	1.25	...	...
0407−658	1	...	QSO?	462.0	2.2	21.7	3.0	4.7	0.7	...	1.53	...	...
0409−752	1	...	GAL	984.0	4.8	73.3	11.7	7.5	1.2	...	1.15	...	...
0413−210	2	0.80700	QSO	856.1	2.3	20.4	4.2	2.4	0.5	0.52	0.39	27.57	1.15
0518−458	1	...	GAL	791.0	5.0	<24.5	4.9	<3.1	0.6	...	2.27	...	...
0602−319	1	0.45200	QSO	416.0	1.4	18.1	2.8	4.4	0.7	0.67	0.84	27.03	1.00
0604−203	2	0.16400	GAL	172.5	1.4	13.3	2.3	7.7	1.3	0.81	1.37	26.07	0.40
0614−349	1	0.32900	GAL	494.1	1.7	17.8	4.0	3.6	0.8	0.58	0.77	26.78	<0.08
0806−103	2	0.10700	GAL	388.0	3.0	18.4	4.7	4.7	1.2	0.40	1.10	25.87	4.10
0834−196	2	...	GAL?	410.0	1.4	12.3	2.8	3.0	0.7	0.89	1.00	...	0.16
0842−754	1	...	QSO	305.0	5.0	<26.5	5.3	<8.7	1.7	...	1.17	...	...
0858−279	2	2.15200	QSO	1477.0	1.6	105.5	6.7	7.1	0.5	0.02	−0.03	28.15	<0.15
0915−118	2	0.05470	GAL	1851.4	3.3	222.4	18.8	12.0	1.0	0.84	1.54	26.23	0.04
0941−080	2	...	GAL	371.5	2.1	<12.7	2.5	<3.4	0.7	0.72	0.82	...	0.09
1015−314	1	...	GAL	451.3	1.6	37.8	3.4	8.4	0.8	0.79	0.86	...	0.08
1017−426	1	...	QSO	249.9	0.7	21.2	1.8	8.5	0.7	...	1.24	...	...
1143−483	1	...	GAL	419.7	1.9	<15.8	3.2	<3.8	0.8	...	0.82	...	...
1151−348	1	0.25800	QSO	996.9	1.8	27.0	5.0	2.7	0.5	0.61	0.79	26.89	<0.04
1221−423	1	...	GAL	359.5	1.2	18.9	1.9	5.3	0.5	...	0.80	...	...
1229−021	2, 3	1.04500	QSO	679.7	2.1	26.2	6.9	3.8	1.0	0.33	0.34	27.60	0.58
1239−044	2, 3	0.48000	GAL	186.0	3.0	<17.5	3.5	<9.4	1.9	1.01	1.29	27.05	0.45
1245−197	2	1.27500	QSO	767.7	1.6	16.9	4.3	2.2	0.6	0.56	0.90	28.22	0.33
1246−410	1	...	GAL	209.1	0.9	23.4	2.7	11.2	1.3	...	1.44	...	...
1306−095	2, 3	0.46400	GAL?	841.0	3.0	54.5	13.9	6.5	1.7	0.61	0.63	27.24	0.28
1308−220	2	...	EF	215.8	1.3	21.6	3.4	10.0	1.6	0.99	1.28	...	0.34
1318−434	1	...	GAL	523.4	1.5	<12.9	2.6	<2.5	0.5	...	1.03	...	...
1320−446	1	...	QSO	283.1	0.6	8.9	1.3	3.2	0.5	...	1.01	...	...
1322−428	1	...	GAL	6609.9	6.9	93.0	3.5	1.4	0.1	...	−0.60	...	...
1331−098	2, 3	0.08100	GAL	70.0	4.0	<22.5	4.5	<32.1	6.5	...	2.25	...	...
1333−337	1	0.01290	GAL	269.7	1.7	16.8	2.3	6.2	0.9	...	2.47	...	...
1335−061	2, 3	0.62500	QSO	146.0	3.0	<13.5	2.7	<9.2	1.9	0.83	1.48	27.27	2.24
1355−416	1	...	QSO	194.5	1.7	11.3	1.9	5.8	1.0	...	1.53	...	...
1524−136	2, 3	1.68700	QSO	461.4	3.7	20.5	7.6	4.4	1.6	0.66	0.74	28.19	0.22
1637−771	1	...	GAL	430.8	1.7	<18.0	3.6	<4.2	0.8	...	1.44	...	...
1733−565	1	...	GAL	342.5	1.7	14.3	2.4	4.2	0.7	...	1.76	...	...

Table 5. continued.

(1) name	(2) dates	(3) z	(4) type	(5) I	(6) σ_I	(7) F_p	(8) σ_F	(9) $\Pi_{18.5}$	(10) σ_Π	(11) $\alpha_{1.4}^{5}$	(12) $\alpha_{5}^{18.5}$	(13) $\log L_5$	(14) $\Pi_{1.4}$
1740−517	1	...	GAL?	1361.8	1.6	16.5	3.1	1.2	0.2	...	0.61	...	...
1814−637	1	...	GAL	1584.3	2.2	<13.0	2.6	<0.8	0.2	...	0.79	...	...
1829−718	1	...	NO ID	258.3	0.5	10.0	1.2	3.9	0.4	...	1.05	...	...
1934−638	1, 2, 3	...	GAL	1166.3	0.3	8.6	0.5	0.7	0.0	...	1.28	...	...
1938−155	3	0.45200	GAL	495.1	7.2	39.9	9.0	8.1	1.8	0.86	1.15	27.32	3.32
2008−068	3	...	GAL	399.7	6.2	28.5	7.0	7.1	1.8	0.50	0.94	...	0.28
2032−350	1	...	GAL?	468.0	2.0	17.9	6.0	3.8	1.3	0.84	1.08	...	5.75
2044−027	3	0.94200	QSO	382.0	6.0	<27.0	5.4	<7.1	1.4	0.63	0.75	27.58	0.35
2053−201	3	0.15600	GAL	109.0	7.0	38.4	8.1	35.2	7.5	0.77	1.70	26.01	<0.14
2135−209	3	0.63500	GAL	479.9	7.1	39.4	10.0	8.2	2.1	0.69	0.89	27.43	<0.06
2140−816	1	...	NO ID	149.8	1.4	12.3	1.9	8.2	1.3	...	1.451	...	...
2149−287	3	...	NO ID	403.6	8.1	43.3	9.4	10.7	2.3	0.585	0.929	...	2.67
2150−520	1	...	QSO?	268.9	0.6	11.2	1.8	4.2	0.7	...	1.150	...	...
2226−411	1	...	QSO	295.2	0.8	25.4	1.5	8.6	0.5	...	0.991	...	...
2250−412	1	...	GAL	281.3	0.7	13.7	2.0	4.9	0.7	...	1.187	...	...
2252−530	1	...	GAL?	279.2	0.6	17.5	1.3	6.3	0.5	...	0.983	...	...
2317−277	2, 3	...	GAL	67.0	2.0	<32.0	6.4	<47.8	9.6	0.398	2.267	...	16.20
2323−407	1	...	GAL	221.5	0.8	40.5	1.5	18.3	0.7	...	1.218	...	...
2331−417	1	...	GAL	290.0	1.4	12.8	2.3	4.4	0.8	...	1.301	...	...

Table 6. Summary of observed and derived quantities for flat-spectrum sources. Same columns as in Table 5.

(1) name	(2) dates	(3) z	(4) type	(5) I	(6) σ_I	(7) F_p	(8) σ_F	(9) $\Pi_{18.5}$	(10) σ_Π	(11) $\alpha_{1.4}^{5}$	(12) $\alpha_{5}^{18.5}$	(13) $\log L_5$	(14) $\Pi_{1.4}$
0003−066	2,3	0.34700	QSO	2561.3	11.9	29.8	13.4	1.2	0.5	0.25	−0.41	26.82	2.7
0047−579	1	1.79700	QSO	1643.0	2.8	77.5	7.8	4.7	0.5	...	0.29	...	...
0048−097	2,3	...	QSO	1397.1	4.9	37.2	7.7	2.7	0.5	−0.69	0.26	...	3.1
0056−572	1	...	QSO	580.1	3.1	<20.1	4.0	<3.5	0.7	...	0.48	...	...
0112−017	2,3	1.38100	QSO	777.6	5.4	30.5	6.9	3.9	0.9	−0.08	0.33	27.72	1.0
0113−118	2,3	0.67200	QSO	1430.1	2.9	28.4	7.6	2.0	0.5	−0.06	0.23	27.41	3.9
0122−003	2,3	1.07000	GAL	1721.5	3.4	60.0	10.7	3.5	0.6	0.17	−0.25	27.63	4.4
0130−171	2,3	1.02200	QSO	1614.4	8.4	36.7	6.8	2.3	0.4	−0.14	−0.36	27.41	1.3
0131−522	1	...	QSO	794.5	1.8	24.7	4.5	3.1	0.6	...	0.32	...	...
0138−097	2,3	0.50100	QSO	922.8	3.0	59.4	11.3	6.4	1.2	−0.48	0.21	...	1.5
0202−172	2	1.74000	QSO	1087.3	4.8	<20.3	4.1	<1.9	0.4	−0.09	0.18	27.93	2.6
0208−512	1	1.00300	BL/QSO	2913.7	7.1	99.2	9.9	3.4	0.3	...	0.09	...	...
0238−084	2,3	0.00500	QSO	1012.5	8.2	<24.4	4.9	<2.4	0.5	−0.35	0.26	...	0.3
0302−623	1	...	QSO	1870.5	2.4	61.8	10.9	3.3	0.6	...	−0.21	...	...
0308−611	1	...	QSO	1215.5	1.0	18.9	4.1	1.6	0.3	...	0.08	...	...
0332−403	1	1.44500	QSO	1786.4	1.9	63.9	9.1	3.6	0.5	...	0.27	...	...
0336−019	2,3	0.85200	QSO	4485.9	7.8	147.1	21.7	3.3	0.5	−0.13	−0.34	27.74	3.2
0400−319	1	...	GAL	885.6	3.2	22.0	5.8	2.5	0.7	−0.34	0.13	...	1.8
0402−362	1	1.41700	QSO	3180.9	3.0	42.2	4.1	1.3	0.1	−0.14	−0.63	27.78	0.4
0403−132	2	0.57100	QSO	2292.2	3.0	36.6	5.6	1.6	0.2	0.30	0.17	27.53	2.1
0405−385	1	1.28500	QSO	1636.5	2.9	24.9	5.7	1.5	0.3	−0.18	−0.31	27.59	1.1
0405−123	2	0.57400	BL/QSO	1430.6	3.3	23.8	5.8	1.7	0.4	0.31	0.24	27.37	1.1
0414−189	2	1.53600	QSO	913.0	2.8	25.1	4.4	2.7	0.5	−0.06	0.29	27.85	0.5
0420−014	2	0.91500	QSO	7912.8	13.0	85.5	12.5	1.1	0.2	0.49	−1.29	27.67	1.2
0426−380	1	1.03000	BL/QSO	1056.3	2.2	61.5	6.2	5.8	0.6	−0.36	0.07	...	7.0
0434−188	2	2.70200	QSO	423.9	2.1	13.7	3.6	3.2	0.8	−0.42	0.81	27.98	0.7
0437−454	1	...	QSO	1127.2	1.4	36.5	5.1	3.2	0.5	...	0.17	...	...
0438−436	1	2.85200	QSO	3926.9	3.0	97.3	2.4	2.5	0.1	...	0.43	...	...
0440−003	2	0.84400	QSO	1214.8	3.4	22.6	6.4	1.9	0.5	−0.30	0.58	27.65	0.6
0454−810	1	0.44400	QSO	1574.3	3.5	40.7	7.3	2.6	0.5	...	−0.09	...	...
0451−282	2	2.55900	QSO	1746.6	1.6	46.9	7.8	2.7	0.4	0.09	0.19	28.50	0.8
0454−463	1	0.85800	QSO	3599.6	2.3	27.8	3.8	0.8	0.1	...	−0.33	...	...
0454−234	2	1.00300	QSO	5389.8	4.9	157.5	4.3	2.9	0.1	−0.13	−0.73	27.71	3.2

Table 6. continued.

(1)	(2)	(3)	(4)	(5)	(6)	(7)	(8)	(9)	(10)	(11)	(12)	(13)	(14)
name	dates	z	type	I	σ_I	$F_{\rm p}$	$\sigma_{\rm F}$	$\Pi_{18.5}$	σ_Π	$\alpha_{1.4}^{5}$	$\alpha_{5}^{18.5}$	$\log L_5$	$\Pi_{1.4}$
0458−020	2	2.28600	QSO	1568.7	3.5	24.5	6.8	1.6	0.4	0.20	0.07	28.37	0.5
0506−612	1	1.09300	BL/QSO	2436.4	2.0	50.2	9.5	2.1	0.4	...	−0.26	...	...
0511−220	2	1.29600	QSO	768.5	2.2	34.2	5.7	4.5	0.7	−0.55	0.40	27.54	0.9
0514−459	1	0.19400	QSO	886.8	2.1	35.9	7.1	4.0	0.8	...	0.13	...	...
0524−460	1	1.47900	QSO	523.9	2.6	15.9	3.3	3.0	0.6	...	0.50	...	...
0528−250	2	2.76500	QSO	469.3	2.7	14.4	2.7	3.1	0.6	0.00	0.69	28.21	0.6
0537−441	1	0.89600	QSO	10682.9	3.9	290.8	2.7	2.7	0.0	...	−0.75	...	...
0537−286	2	3.11900	QSO	865.7	3.0	20.1	3.9	2.3	0.5	−0.13	0.12	28.16	0.6
0539−057	2	0.83900	QSO	782.7	2.8	21.0	4.1	2.7	0.5	−0.44	0.52	27.38	4.3
0605−085	2	0.87200	BL/QSO	1958.8	3.2	58.6	2.8	3.0	0.1	−0.47	0.44	27.75	2.2
0606−223	2	1.92600	QSO	949.1	1.8	23.6	4.6	2.5	0.5	−0.56	0.29	27.79	1.9
0607−157	2	0.32400	QSO	5999.5	7.5	287.2	5.1	4.8	0.1	0.32	−0.91	26.86	1.3
0637−752	1	0.65400	QSO	4777.8	4.4	156.8	3.0	3.3	0.1	...	0.15	...	...
0642−349	1	2.16500	QSO	321.5	2.1	16.5	3.0	5.1	0.9	−0.27	0.88	27.86	1.0
0743−006	2	0.99400	QSO	1615.1	3.7	35.1	5.1	2.2	0.3	−0.86	0.16	27.47	0.4
0805−077	2	1.83700	QSO	1659.5	2.0	21.0	6.2	1.3	0.4	0.33	−0.35	28.04	1.4
0834−201	2	2.75200	QSO	4383.0	5.8	81.7	3.9	1.9	0.1	−0.49	−0.12	28.43	0.3
0859−140	2	1.33900	QSO	1190.3	1.5	38.4	3.5	3.2	0.3	0.18	0.50	28.08	3.2
0919−260	2	2.30000	QSO	1442.5	2.1	23.0	4.7	1.6	0.3	−0.01	−0.06	28.14	0.9
1032−199	2	2.19800	QSO	1260.3	2.4	26.7	6.5	2.1	0.5	−0.18	−0.07	27.97	5.3
1045−188	2	0.59500	QSO	1625.2	2.1	36.4	7.7	2.2	0.5	0.01	−0.27	27.10	2.3
1057−797	1	...	QSO	2638.0	1.9	100.1	8.4	3.8	0.3	...	−0.37	...	...
1104−445	1	1.59800	QSO	2273.0	2.4	27.7	3.5	1.2	0.2	...	−0.07	...	...
1116−462	1	0.71300	BL/QSO	963.8	2.3	39.8	1.3	4.1	0.1	...	0.25	...	...
1127−145	2	1.18700	QSO	2926.2	2.2	116.3	2.7	4.0	0.1	−0.12	0.61	28.34	4.0
1143−245	2	1.95000	QSO	691.3	3.3	<17.7	3.5	<2.6	0.5	0.15	0.40	28.06	1.7
1144−379	1	1.04800	QSO	4431.6	5.8	323.7	2.2	7.3	0.0	0.08	−0.77	...	2.2
1145−071	2	1.34200	QSO	809.9	1.7	22.2	3.6	2.7	0.4	−0.41	0.33	27.60	1.9
1148−001	2	1.98200	QSO	972.2	1.0	20.6	4.6	2.1	0.5	0.29	0.51	28.35	4.6
1202−262	2	0.78900	NO ID	509.3	1.5	<11.5	2.3	<2.3	0.5	0.36	0.54	27.37	1.1
1213−172	2	...	GAL	1897.1	2.5	41.3	3.9	2.2	0.2	0.09	−0.19	...	1.1
1237−101	2,3	0.75300	QSO	1032.6	5.4	23.6	7.6	2.3	0.7	0.11	0.18	27.37	2.9
1243−072	2,3	1.28600	QSO	712.1	1.0	24.5	6.7	3.4	0.9	...	0.28	...	...
1244−255	2	0.63300	GAL	1848.1	3.1	60.6	14.4	3.3	0.8	−0.12	−0.23	27.20	3.6
1253−055	1,2,3	0.53600	QSO	28043.5	12.3	1648.5	1.7	5.9	0.0	−0.33	−0.48	28.07	2.6
1255−316	1	1.92400	QSO	2000.6	3.5	86.9	13.7	4.3	0.7	−0.32	−0.11	27.99	5.3
1302−102	2,3	0.28600	QSO	827.0	2.0	26.4	7.4	3.2	0.9	−0.39	0.26	26.48	0.4
1313−333	1	1.21000	BL/QSO	1457.6	3.0	33.2	8.0	2.3	0.5	−0.04	−0.05	27.69	1.1
1334−127	2,3	0.53900	QSO	7107.4	6.8	88.4	23.0	1.2	0.3	0.14	−0.88	27.34	2.3
1352−104	2,3	0.33200	QSO	1659.4	2.0	35.1	10.9	2.1	0.7	−0.21	−0.37	26.56	4.3
1354−152	2	1.89000	QSO	999.8	1.3	21.4	6.0	2.1	0.6	−0.63	0.32	27.78	2.0
1406−076	2,3	1.49400	QSO	1792.3	4.9	35.2	11.3	2.0	0.6	−0.35	−0.38	27.62	3.1
1424−418	1	1.52200	QSO	2923.3	2.1	25.6	4.5	0.9	0.2	...	0.05	...	...
1451−375	1	0.31400	QSO	2004.8	3.1	78.1	5.8	3.9	0.3	−0.54	−0.04	26.75	3.0
1504−166	3	0.87600	QSO	1498.6	10.0	<47.3	9.5	<3.2	0.6	0.24	0.21	27.70	0.3
1508−055	2,3	1.19100	BL/QSO	1272.2	6.2	37.3	11.9	2.9	0.9	0.30	0.49	28.05	1.2
1510−089	2,3	0.36100	QSO	2527.6	5.7	63.1	18.9	2.5	0.7	−0.10	0.15	27.12	3.4
1514−241	3	0.04860	QSO	2030.1	11.4	86.9	13.4	4.3	0.7	0.01	−0.01	...	5.1
1519−273	3	...	QSO	1632.3	8.8	90.4	6.8	5.5	0.4	−0.59	0.27	...	1.9
1541−828	1	...	GAL	589.7	1.8	15.0	3.1	2.5	0.5	...	0.69	...	...
1549−790	1	0.14900	QSO	1429.2	2.1	<14.8	3.0	<1.0	0.2	...	0.72	...	...
1555+001	2,3	1.77000	QSO	891.5	3.8	<26.3	5.3	<3.0	0.6	−0.55	0.70	27.95	0.9
1610−771	1	1.71000	QSO	2674.3	3.0	46.1	2.0	1.7	0.1	...	0.29	...	...
1619−680	1	1.35400	GAL	724.7	1.4	<14.7	2.9	<2.0	0.4	...	0.72	...	...
1622−253	3	...	QSO	2144.1	19.4	86.7	16.8	4.0	0.8	0.15	−0.02	...	0.5
1718−649	1	0.01450	QSO	3003.2	2.7	18.7	4.4	0.6	0.1	...	0.18	...	...

Table 6. continued.

(1) name	(2) dates	(3) z	(4) type	(5) I	(6) σ_I	(7) F_p	(8) σ_F	(9) $\Pi_{18.5}$	(10) σ_Π	(11) $\alpha_{1.4}^{5}$	(12) $\alpha_{5}^{18.5}$	(13) $\log L_5$	(14) $\Pi_{1.4}$
1741−038	3	1.05700	QSO	4921.9	21.8	77.2	13.6	1.6	0.3	−0.75	−0.22	27.81	0.6
1815−553	1	...	QSO	1097.2	2.2	15.4	3.4	1.4	0.3	...	0.15	...	...
1831−711	1	1.35600	QSO	2221.1	2.1	27.1	4.3	1.2	0.2	...	−0.47	...	...
1903−802	1	0.50000	QSO	614.9	2.0	18.5	3.5	3.0	0.6	...	0.83	...	...
1933−400	1	0.96600	QSO	1162.7	1.5	26.9	3.3	2.3	0.3	−0.30	0.18	27.49	2.8
1936−155	3	1.65700	QSO	966.6	8.1	34.7	9.4	3.6	1.0	−0.80	0.42	27.69	0.8
1936−623	1	...	QSO	531.4	1.4	24.4	4.0	4.6	0.8	...	0.55	...	...
1954−388	1	0.62600	GAL	3810.4	1.8	26.5	6.0	0.7	0.2	−0.25	−0.47	27.34	1.3
1958−179	3	0.65000	QSO	1337.7	6.0	39.7	8.7	3.0	0.6	−0.61	−0.08	27.06	0.7
2000−330	1	3.77700	EF	514.7	1.9	<13.3	2.7	<2.6	0.5	−0.74	0.61	27.91	<0.6
2005−489	1	0.07100	QSO	1345.5	1.3	<15.9	3.2	<1.2	0.2	...	−0.06	...	...
2008−159	3	1.18000	QSO	2245.9	7.5	46.7	9.3	2.1	0.4	−0.73	−0.36	27.45	1.3
2052−474	1	1.49100	QSO	739.1	1.5	12.3	2.8	1.7	0.4	...	0.93	...	...
2106−413	1	1.05470	QSO	1895.0	2.8	29.7	4.5	1.6	0.2	...	0.16	...	...
2126−158	3	3.26600	QSO	933.5	10.9	36.9	9.5	4.0	1.0	−0.60	0.24	27.98	<0.4
2128−123	3	0.50100	QSO	3390.8	16.8	86.6	21.7	2.6	0.6	−0.12	−0.37	27.20	2.0
2131−021	3	0.55700	QSO	2272.8	17.9	79.7	20.0	3.5	0.9	−0.17	−0.05	...	1.2
2142−758	1	1.13900	QSO	687.9	2.2	68.4	10.5	9.9	1.5	...	0.49	...	...
2155−152	3	0.67200	QSO	2505.5	17.1	60.5	14.7	2.4	0.6	0.42	−0.26	27.48	4.0
2203−188	2,3	0.61900	QSO	2200.0	11.6	85.8	11.5	3.9	0.5	0.29	0.52	27.78	0.2
2204−540	1,3	1.20600	QSO	1306.6	2.2	86.1	2.0	6.6	0.2	...	0.46	...	...
2206−237	2,3	0.08700	QSO	340.6	2.5	24.6	3.8	7.2	1.1	0.53	0.83	...	0.2
2210−257	2,3	1.83300	QSO	609.1	15.2	29.3	7.6	4.8	1.3	0.11	0.41	27.94	1.4
2216−038	3	0.90100	QSO	2571.6	13.5	66.9	17.5	2.6	0.7	0.30	−0.41	27.62	0.7
2223−052	3	1.40400	QSO	8394.5	10.8	359.7	10.8	4.3	0.1	0.39	−0.47	28.49	4.5
2227−088	3	1.56100	QSO	1570.5	8.1	<40.2	8.0	<2.6	0.5	−0.47	0.09	27.81	1.3
2243−123	3	0.63000	QSO	2043.7	9.8	48.8	16.4	2.4	0.8	−0.20	0.13	27.43	1.4
2345−167	2,3	0.57600	QSO	2747.7	5.1	46.8	5.4	1.7	0.2	−0.25	0.21	27.53	2.8
2353−686	1,3	1.71600	QSO	785.4	0.9	16.4	3.4	2.1	0.4	...	0.25	...	...
2354−117	3	0.96000	QSO	1197.1	7.2	54.0	12.3	4.5	1.0	0.16	0.16	27.62	1.5
2355−534	1,3	1.00600	QSO	1602.1	2.7	51.9	6.9	3.2	0.4	...	−0.04	...	...
2255−282	2,3	0.92600	QSO	11226.5	20.3	379.2	6.7	3.4	0.1	−0.27	−1.40	27.55	1.0
2311−452	1,3	2.88400	QSO	585.6	1.6	28.1	4.5	4.8	0.8	...	0.70	...	...
2326−477	1,3	1.30600	GAL	1571.0	2.8	23.1	3.6	1.5	0.2	...	0.30	...	...
2329−162	2,3	1.15500	QSO	1964.4	8.1	99.2	19.7	5.0	1.0	0.18	−0.47	27.63	1.1
2331−240	2,3	0.04770	QSO	1095.7	3.5	25.8	5.8	2.4	0.5	−0.26	−0.00	...	1.0
2333−528	1,3	...	QSO	1113.9	0.9	23.3	3.3	2.1	0.3	...	0.07	...	...

References

Aller, M. F., Aller, H. D., Hughes, P. A., & Latimer, G. E. 1999, ApJ, 512, 601

Condon, J. J., Cotton, W. D., Greisen, E. W., et al. 1998, AJ, 115, 1693

De Zotti, G., Gruppioni, C., Ciliegi, P., Burigana, C., & Danese, L. 1999, NewA, 4, 481

Feigelson, E. D., & Nelson, P. I., 1985, ApJ, 293, 192

Isobe, T., & Feigelson, E. D., 1990, BAAS, 22, 917

Isobe, T., Feigelson, E. D., & Nelson, P. I., 1986, ApJ, 306, 490

Jones, T. W., Rudnick, L., Aller, H. D., et al. 1985, ApJ, 290, 627

Klein, U., Mack, K.-H., Gregorini, L., & Vigotti, M., 2003, A&A, 406, 579

Kogut, A., Spergel, D. N., Barnes, C., et al. 2003, ApJS, 148, 161

Kovac, J. M., Leitch, E. M., Pryke, C., et al. 2002, Nature, 420, 772

Kühr, H., Witzel, A., Pauliny-Toth, I. I. K., & Nauber U. 1981, A&AS, 45, 367

Mesa, D., Baccigalupi, C., De Zotti, G., et al. 2002, A&A, 396, 463

Nartallo, R., Gear, W. K., Murray, A. G., Robson, E. I., & Hough, J. H. 1998, MNRAS, 297, 667

Okudaira, A., Tabara, H., Kato, T., & Inoue, M. 1993, PASJ, 45, 153

Pentericci, L., Van Reeven, W., Carilli, C. L., Röttgering, H. J. A., & Miley, G. K. 2000, A&AS, 145, 121

Rudnick, L., Jones, T. W., Aller, H. D., et al. 1985, ApJS. 57, 693

Saikia, D. J., & Salter, C. J. 1988, ARA&A, 26, 93

Sazhin, M. V., & Korolëv, V. A. 1985, Sov. Astron. Lett., 11, 204

Sault, R. J., Teuben, P. J., & Wright, M. C. H, A retrospective view of Miriad in Astronomical Data Analysis Software and Systems, ed. R. Shaw, H. E. Payne, & J. J. E. Haynes, ASP Conf. Ser., 77, 433

Stickel, M., Meisenheimer, K., & Kühr, H., 1994, A&AS, 105, 211